Supporting Information

Amorphous Mn_2SiO_4: A potential manganese phase in the stagnant slab

Zhilin Ye [1,2], Jingui Xu [1, 3,*], Dawei Fan [1,*], Dongzhou Zhang [3], Wenge Zhou [1], Hongsen Xie [1]

1 Key Laboratory of High-Temperature and High-Pressure Study of the Earth's Interior, Institute of Geochemistry, Chinese Academy of Sciences, Guiyang, Guizhou 550081, China

2 University of Chinese Academy of Sciences, Beijing 100049, China

3 Hawaii Institute of Geophysics and Planetology, School of Ocean and Earth Science and Technology, University of Hawaii at Manoa, Honolulu, Hawaii 96822, USA

* Corresponding authors:

E-mail addresses: fandawei@vip.gyig.ac.cn (D. Fan), xujingui1990@126.com (J. Xu)

Figure S1-S6

Table S1-S7

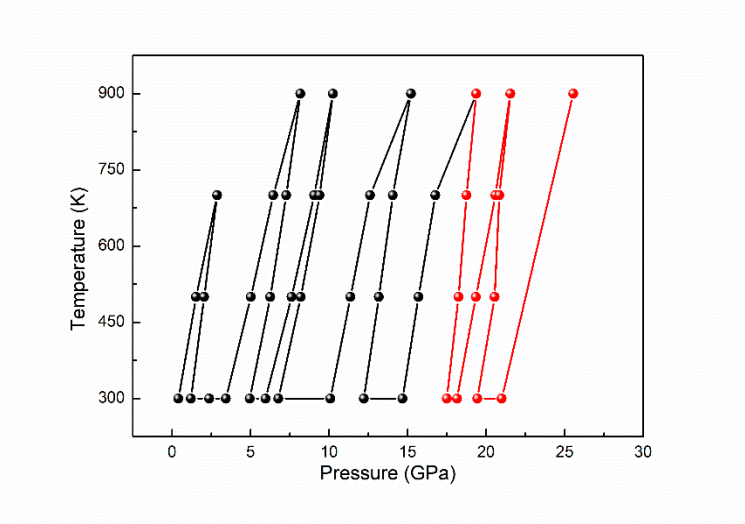

Figure S1. High-pressure and high-temperature experimental *P-T* path for tephroite. The solid circles represent the collection points of the single-crystal diffraction data. The black and red circles indicate α-tephroite and amorphous tephroite, respectively.

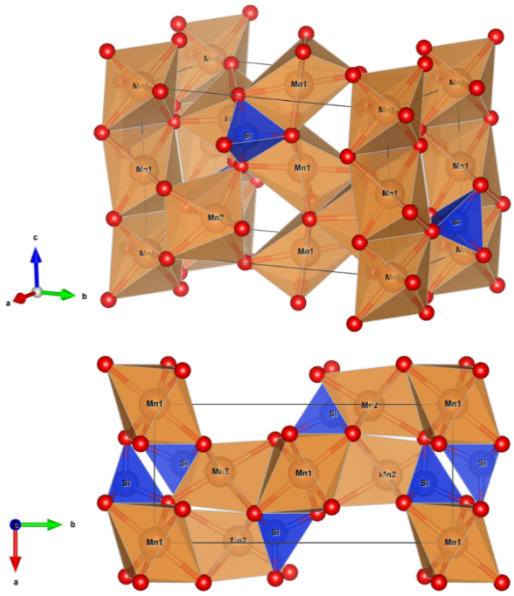

Figure S2. Crystal structure of Tephroite at ambient conditions.

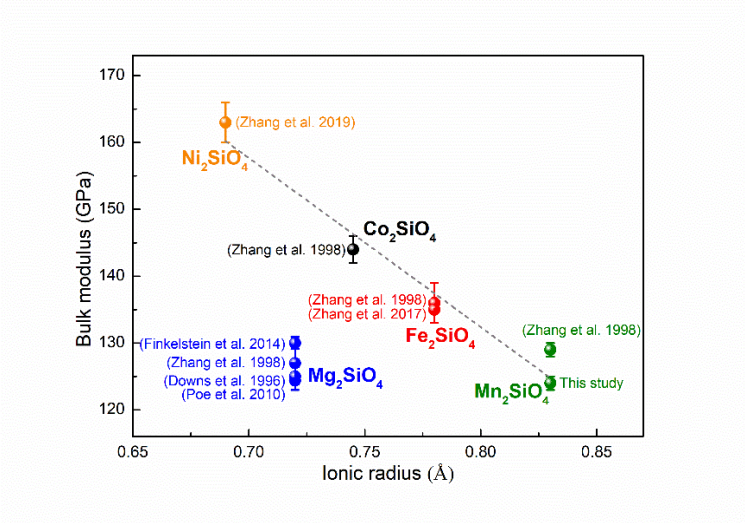

Figure S3. Variation in bulk moduli of end-member olivine (Ni, Co, Fe, Mn, Mg)$_2$SiO$_4$ with ionic radius. The bulk moduli of olivine from previous studies are shown for comparison (Downs et al. 1996; Zhang 1998; Poe et al. 2010; Finkelstein et al. 2014; Zhang et al. 2017, 2019). The gray dashed line represents the linear fit.

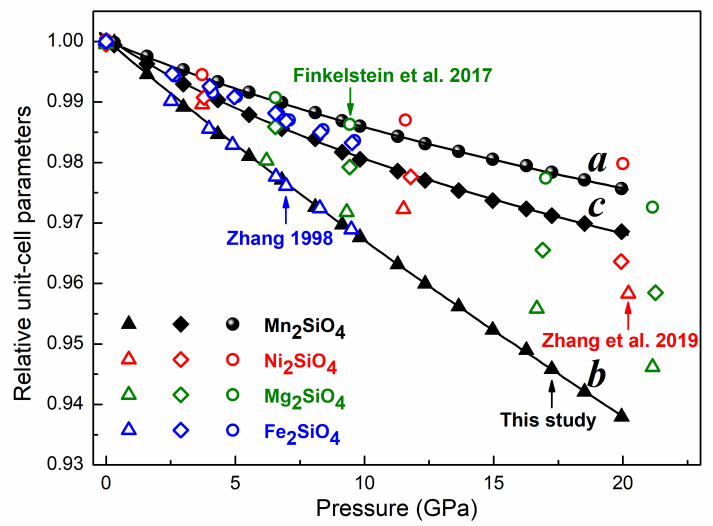

Figure S4. Pressure dependence of the relative unit-cell parameters *a*, *b*, *c* of Tephroite and other end-member olivines at room temperature.

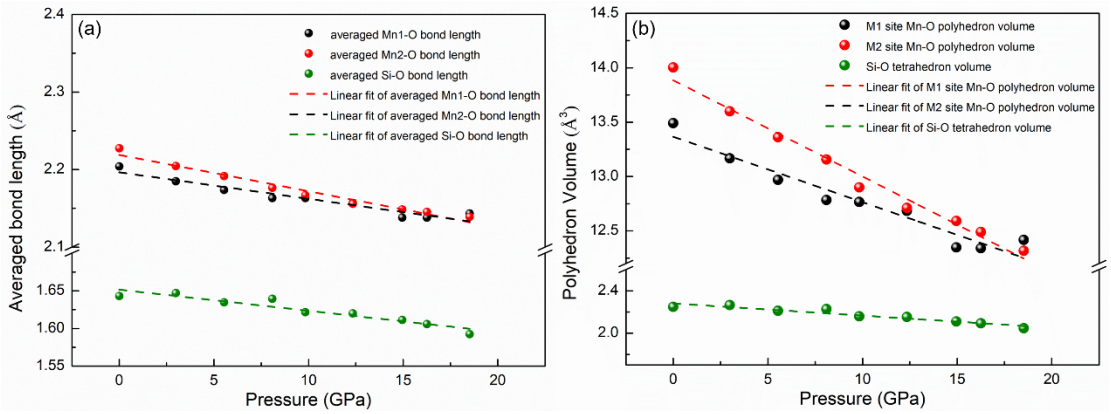

Figure S5. Pressure independence of averaged bond length (a) and polyhedron volume (b) in this study. The dashed lines represent the linear fitting.

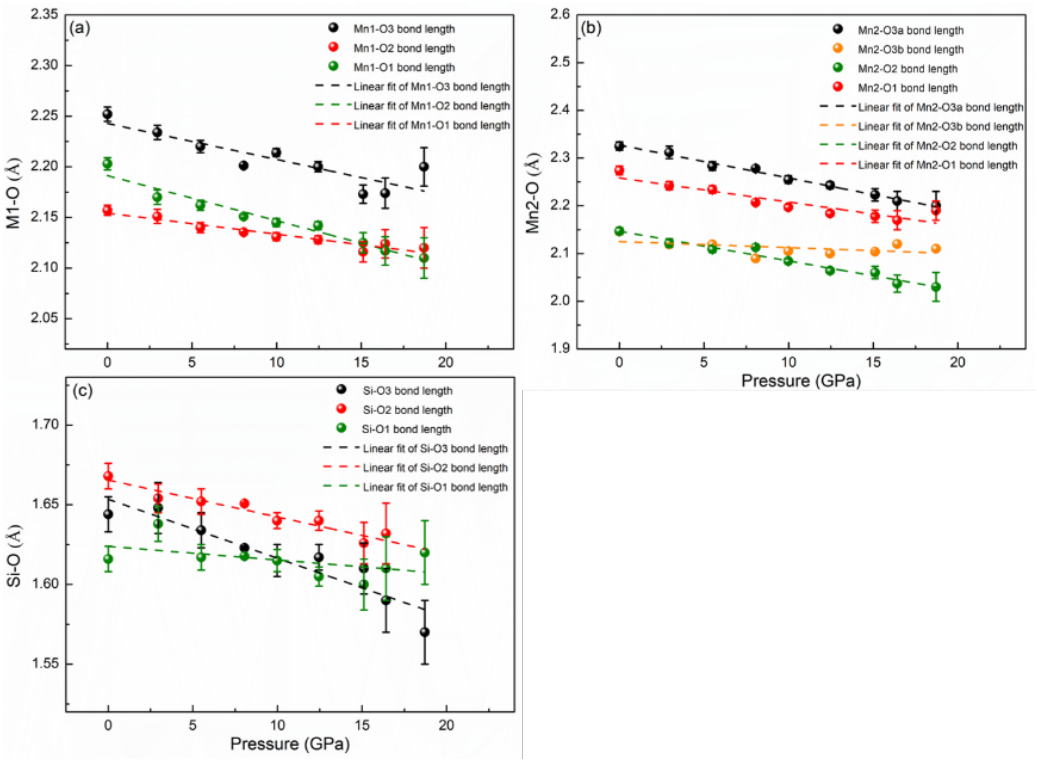

Figure S6. Pressure independence of bond length in this study: (a) Mn1-O, (b) Mn2-O, (c) Si-O. The dashed lines represent the linear fitting.

Table S1. Chemical compositions of tephroite based on the average of at least 5-point electron microprobe analyses

Oxide (wt.%)	Tephroite
SiO_2	29.59(54)
TiO_2	0.02(1)
Al_2O_3	0.02(2)
Cr_2O_3	-
FeO	0.51(7)
MnO	72.39(38)
MgO	0.01(0)
CaO	0.01(2)
Na_2O	0.01(1)
K_2O	-
Total	102.58 (66)

- Below the detection limit

Table S2. Lattice parameters and unit-cell volumes of tephroite at room temperature and high pressure (a) and high temperature and high pressure (b).

P (GPa)	*T* (K)	*a* (Å)	*b* (Å)	*c* (Å)	*V* (Å^3)
(a) room temperature and high pressure					
0.0001	300	4.903(1)	10.599(1)	6.258(3)	325.22(13)
0.32(2)	300	4.893(2)	10.597(1)	6.255(1)	324.28(11)
1.58(10)	300	4.880(1)	10.542(1)	6.235(1)	320.77(8)
2.99(17)	300	4.880(1)	10.484(1)	6.214(1)	317.91(6)
4.33(17)	300	4.868(2)	10.437(1)	6.198(1)	314.85(14)
5.54(16)	300	4.857(2)	10.398(2)	6.182(1)	312.22(11)
6.79(16)	300	4.846(1)	10.357(1)	6.168(1)	309.57(6)
8.09(20)	300	4.841(3)	10.309(3)	6.157(1)	307.29(17)
9.13(16)	300	4.831(2)	10.278(2)	6.144(1)	305.06(8)
9.83(2)	300	4.829(1)	10.256(1)	6.136(1)	303.92(6)
11.28(23)	300	4.821(2)	10.208(1)	6.124(1)	301.40(8)
12.35(16)	300	4.818(1)	10.174(1)	6.114(1)	299.71(4)
13.65(14)	300	4.811(1)	10.135(1)	6.104(1)	297.58(4)
14.96(21)	300	4.806(1)	10.094(1)	6.093(1)	295.60(5)
16.26(21)	300	4.795(1)	10.058(1)	6.085(1)	293.48(6)
17.25(21)	300	4.794(1)	10.025(1)	6.078(1)	292.11(6)
18.52(23)	300	4.786(1)	9.985(1)	6.070(1)	290.09(5)
19.95(18)	300	4.778(2)	9.941(1)	6.061(1)	287.88(7)
(b) high temperature and high pressure					
0.41(2)	300	4.895(1)	6.125(2)	10.855(1)	324.07(3)
1.21(1)	300	4.888(1)	6.238(1)	10.546(1)	321.61(4)
2.37(5)	300	4.879(2)	6.221(2)	10.499(1)	318.67(4)
3.44(1)	300	4.867(1)	6.205(1)	10.449(1)	315.59(4)
4.95(1)	300	4.858(2)	6.191(2)	10.401(1)	312.85(5)
5.95(1)	300	4.851(2)	6.175(2)	10.361(1)	310.35(4)
6.78(4)	300	4.846(1)	6.167(1)	10.327(1)	308.62(4)
10.09(2)	300	4.823(1)	6.130(1)	10.218(1)	302.11(4)
12.21(3)	300	4.814(1)	6.109(1)	10.135(1)	298.04(4)

14.68(11)	300	4.799(2)	6.083(2)	10.060(1)	293.66(6)
1.53(4)	500	4.895(2)	6.252(1)	10.575(1)	323.61(5)
2.04(4)	500	4.888(2)	6.243(1)	10.546(1)	321.84(4)
5.02(8)	500	4.866(2)	6.203(2)	10.434(1)	314.9(5)
6.26(8)	500	4.855(2)	6.185(2)	10.376(1)	311.64(4)
7.61(16)	500	4.845(2)	6.166(2)	10.325(1)	308.43(5)
8.20(18)	500	4.843(2)	6.164(2)	10.307(1)	307.69(5)
11.36(9)	500	4.822(2)	6.129(2)	10.198(1)	301.38(4)
13.17(11)	500	4.813(1)	6.110(1)	10.131(1)	297.88(4)
15.70(1)	500	4.798(2)	6.087(2)	10.049(1)	293.50(4)
2.87(7)	700	4.892(3)	6.246(2)	10.551(1)	322.42(8)
6.44(1)	700	4.860(2)	6.198(2)	10.406(1)	313.47(6)
7.28(9)	700	4.854(2)	6.187(2)	10.372(1)	311.44(6)
9.06(10)	700	4.841(2)	6.167(2)	10.309(1)	307.75(5)
9.40(12)	700	4.841(2)	6.160(1)	10.292(1)	306.91(4)
12.61(7)	700	4.821(2)	6.127(2)	10.181(1)	300.72(4)
14.06(18)	700	4.811(2)	6.113(2)	10.126(1)	297.78(5)
16.77(8)	700	4.797(2)	6.088(2)	10.034(1)	293.03(4)
8.17(8)	900	4.858(3)	6.188(3)	10.371(1)	311.77(10)
10.25(5)	900	4.840(3)	6.165(2)	10.288(1)	306.94(10)
15.22(4)	900	4.809(3)	6.112(2)	10.108(1)	297.12(8)

Numbers in parenthesis represent standard deviations

Table S3. Structure refinement details, fractional coordinates and isotropic displacement parameters for Tephroite at different pressures

P (GPa)	Final R indices [$I > 2\sigma(I)$]	Number total reflections/ unique reflections/ refined parameters	Atom	*x*	*y*	*z*	U_{iso}
0.0001	R1=0.045 wR_2=0.117	321/82/18 [R(int)=0.0477]	Mn1	0.000000	0.000000	0.000000	0.0074(12)
			Mn2	0.9880(4)	0.28026(15)	0.250000	0.0047(12)
			Si	0.4280(8)	0.0968(3)	0.250000	0.0040(13)
			O1	0.7575(14)	0.0941(8)	0.250000	0.004(2)
			O2	0.2139(15)	0.4538(6)	0.250000	0.004(2)
			O3	0.2878(13)	0.1639(6)	0.040(2)	0.0065(19)
2.99(17)	R1=0.071 wR_2=0.191	735/158/18 [R(int)=0.0712]	Mn1	0.000000	0.000000	0.000000	0.0140(6)
			Mn2	0.9860(4)	0.27995(14)	0.250000	0.0112(6)
			Si	0.4269(9)	0.0966(3)	0.250000	0.0128(9)
			O1	0.7625(19)	0.0930(8)	0.250000	0.0115(19)
			O2	0.2126(19)	0.4528(7)	0.250000	0.0113(19)
			O3	0.2865(15)	0.1647(5)	0.038(3)	0.0140(14)
5.54(16)	R1=0.060 wR_2=0.161	735/149/18 [R(int)=0.0632]	Mn1	0.000000	0.000000	0.000000	0.0141(5)
			Mn2	0.9850(3)	0.27969(12)	0.250000	0.0112(5)
			Si	0.4273(7)	0.0971(3)	0.250000	0.0122(7)
			O1	0.7597(14)	0.0923(7)	0.250000	0.0114(16)
			O2	0.2132(15)	0.4523(6)	0.250000	0.0120(16)
			O3	0.2844(12)	0.1654(5)	0.040(2)	0.0134(12)
8.09(20)	R1=0.103 wR_2=0.257	622/123/18 [R(int)=0.0805]	Mn1	0.000000	0.000000	0.000000	0.0149(13)
			Mn2	0.9846(8)	0.2794(3)	0.250000	0.0097(12)
			Si	0.4278(17)	0.0978(6)	0.250000	0.0133(18)
			O1	0.761(3)	0.0927(13)	0.250000	0.008(3)
			O2	0.211(3)	0.4546(12)	0.250000	0.009(3)
			O3	0.282(3)	0.1663(9)	0.035(5)	0.011(3)
9.83(2)	R1=0.033	724/152/18	Mn1	0.000000	0.000000	0.000000	0.0086(4)

	wR_2=0.095	[R(int)=0.0405]	Mn2	0.9830(3)	0.27952(10)	0.250000	0.0048(3)
			Si	0.4264(5)	0.0979(2)	0.250000	0.0051(5)
			O1	0.7603(12)	0.0926(5)	0.250000	0.0045(12)
			O2	0.2121(12)	0.4518(4)	0.250000	0.0025(12)
			O3	0.2848(9)	0.1673(3)	0.0419(19)	0.0064(9)
			Mn1	0.000000	0.000000	0.000000	0.0107(4)
			Mn2	0.9818(3)	0.27945(11)	0.250000	0.0075(4)
12.35(16)	R1=0.048	699/126/18	Si	0.4260(5)	0.0978(2)	0.250000	0.0069(6)
	wR_2=0.072	[R(int)=0.0637]	O1	0.7589(10)	0.0925(5)	0.250000	0.0058(14)
			O2	0.2123(12)	0.4505(5)	0.250000	0.0062(14)
			O3	0.2831(9)	0.1678(4)	0.0417(15)	0.0066(11)
			Mn1	0.000000	0.000000	0.000000	0.0163(8)
			Mn2	0.9808(6)	0.2794(2)	0.250000	0.0104(8)
14.96(21)	R1=0.083	695/113/18	Si	0.4270(11)	0.0972(5)	0.250000	0.0101(12)
	wR_2=0.189	[R(int)=0.0868]	O1	0.759(2)	0.0917(11)	0.250000	0.011(3)
			O2	0.213(2)	0.4503(10)	0.250000	0.010(3)
			O3	0.2802(18)	0.1675(7)	0.043(3)	0.0080(19)
			Mn1	0.000000	0.000000	0.000000	0.0142(14)
			Mn2	0.9801(9)	0.2787(4)	0.250000	0.0088(13)
16.26(21)	R1=0.092	668/107/18	Si	0.4247(18)	0.0964(8)	0.250000	0.009(2)
	wR_2=0.212	[R(int)=0.0909]	O1	0.760(4)	0.0903(19)	0.250000	0.016(5)
			O2	0.212(4)	0.4481(16)	0.250000	0.011(5)
			O3	0.281(3)	0.1669(13)	0.046(5)	0.008(3)
			Mn1	0.000000	0.000000	0.000000	0.015(2)
			Mn2	0.9784(13)	0.2791(5)	0.250000	0.0084(17)
18.52(23)	R1=0.102	644/98/18	Si	0.421(2)	0.0969(10)	0.250000	0.007(3)
	wR_2=0.303	[R(int)=0.102]	O1	0.758(6)	0.088(2)	0.250000	0.017(7)
			O2	0.211(6)	0.448(2)	0.250000	0.010(6)
			O3	0.285(4)	0.1694(16)	0.049(7)	0.008(5)

Table S4. Details of each polyhedron of tephroite under different pressures

P (GPa)	0.0001	2.99(17)	5.54(16)	8.09(20)	9.83(2)	12.35(16)	14.96(21)	16.26(21)	18.52(23)
Mn1 Average bond length (Å)	2.2041	2.1849	2.1737	2.1632	2.1633	2.1569	2.138	2.1379	2.1434
Polyhedral volume (Å^3)	13.491	13.168	12.970	12.784	12.766	12.684	12.348	12.341	12.417
Distortion index	0.01449	0.01495	0.01409	0.01212	0.01554	0.01338	0.01083	0.01211	0.01755
Quadratic elongation	1.0388	1.0373	1.0371	1.037	1.0382	1.0364	1.0367	1.037	1.0382
Bond angle variance	135.0284	130.5926	129.72	129.7995	133.156	127.4935	128.8103	129.7067	132.12
Effective coordination number	5.9304	5.9435	5.9483	5.9627	5.9407	5.956	5.9719	5.9645	5.9239
Mn2 Average bond length (Å)	2.2273	2.2044	2.1914	2.1764	2.1669	2.1558	2.1485	2.1453	2.1391
Polyhedral volume (Å^3)	14.003	13.600	13.362	13.156	12.900	12.712	12.592	12.490	12.318
Distortion index	0.03636	0.03832	0.03452	0.03629	0.03179	0.03146	0.02768	0.02659	0.02767
Quadratic elongation	1.0358	1.0348	1.0344	1.0311	1.0353	1.0347	1.0341	1.0366	1.0403
Bond angle variance	123.4924	119.2335	118.632	107.0648	121.9171	119.8115	118.2012	126.1427	138.4975
Effective coordination number	5.6709	5.6236	5.6985	5.6515	5.7329	5.7244	5.7831	5.7582	5.7369
Si Average bond length (Å)	1.6431	1.6469	1.6345	1.6394	1.6214	1.6199	1.6114	1.6059	1.5925
Polyhedral volume (Å^3)	2.2484	2.2645	2.2102	2.227	2.1584	2.1524	2.1107	2.0934	2.0463
Distortion index	0.00829	0.00267	0.00547	0.0127	0.0057	0.00618	0.00447	0.01109	0.01636
Quadratic elongation	1.0085	1.0082	1.0094	1.0103	1.009	1.009	1.0116	1.0103	1.0088
Bond angle variance	37.6364	34.8516	41.1174	43.0923	38.7379	39.6335	50.5663	42.2048	33.4747
Effective coordination number	3.9816	3.9984	3.9916	3.9764	3.9942	3.9917	3.9956	3.9815	3.9609

Table S5. Equations of state parameters of end-member olivine from single-crystal XRD

Composition	V (Å^3)	K_0 (GPa)	K′$_0$	Medium	P_{max} (GPa)	Reference
Mn_2SiO_4	325.22(13)	124(1)	4.67(29)	Ne	20	This study
	324.3(1)	129(2)	3.0(5)	4:1 meth:eth [a]	10	(Zhang 1998)
	290.14(9)	125(2)	4.0(4)	4:1 meth:eth, Ar, He	17	(Downs et al. 1996)
Mg_2SiO_4	289.3(1)	127(4)	4.2(8)	4:1 meth:eth	10	(Zhang 1998)
	291.15(1)	124.4	4.9	4:1 meth:eth	6.7	(Poe et al. 2010)
	290.1(1)	130.0(9)	4.12(7)	He	50	(Finkelstein et al. 2014)
Fe_2SiO_4	306.9(1)	136(3)	4.1(7)	4:1 meth:eth	10	(Zhang 1998)
		135^{fixed}	4.0(2)	Ne	30.7	(Zhang et al. 2017)
Co_2SiO_4	295.21(7)	144(2)	4.1(5)	4:1 meth:eth	10	(Zhang 1998)
Ni_2SiO_4	283.38(7)	163(3)	4.5(3)	He	42.6	(Zhang et al. 2019)

Numbers in parenthesis represent standard deviations.

[a] 4:1 methanol-ethanol mixture

Table S6. Best-fit volumetric and linear BM3 parameters of the tephroite

Unit-cell parameter	V (Å^3)/ L(Å)	K_0 /M_{l0} (GPa)	K'_0 / $M_l'_0$
Unit-cell volume V	325.22(13)	124(1)	4.67(29)
Lattice parameter a	4.90393(3)	553(15)	32(4)
Lattice parameter b	10.603(1)	273(4)	5.4(5)
Lattice parameter c	6.2626(1)	341(13)	39(4)

Numbers in parenthesis represent standard deviations

Table S7. Frequency of Raman modes, corresponding pressure derivatives, and isothermal mode Grüneisen parameters of tephroite

Symmetry	Frequency, cm^{-1}	$(\partial vi/\partial P)_T$	Υ_{iT}	Mode assignment
A_g	934	4.71(6)	0.62(1)	ν_3
B_{3g}	891	3.21(2)	0.45(0)	ν_3
A_g	841	3.15(5)	0.46(1)	$\nu_1+\nu_3$
A_g	809	3.15(5)	0.48(1)	$\nu_1+\nu_3$
A_g	569	2.73(20)	0.59(1)	ν_4
B_{2g}	550	1.66(18)	0.37(1)	ν_4
A_g	514	1.25(2)	0.3(1)	ν_4
B_{1g}	391	3.58(3)	1.13(1)	ν_2
B_{1g}	317	2.60(6)	1.02(2)	Mix (SiO_4 rot)
A_g	302	4.03(7)	1.64(3)	Mix (SiO_4 rot)
A_g	287	2.98(3)	1.28(2)	M2 translation
B_{3g}	276	2.49(8)	1.12(4)	Mix (M2 trans)
A_g	245	2.25(9)	1.15(5)	M2 translation

Reference：

Birch, F. (1947) Finite Elastic Strain of Cubic Crystals. Physical Review, 71, 809–824.

Downs, R.T., Zha, C.-S., Duffy, T.S., and Finger, L.W. (1996) The equation of state of forsterite to 17.2 GPa and effects of pressure media. American Mineralogist, 81, 51–55.

Fei, Y. (1995) Thermal Expansion. In Mineral Physics & Crystallography: A Handbook of Physical Constants pp. 29–44.

Finkelstein, G.J., Dera, P.K., Jahn, S., Oganov, A.R., Holl, C.M., Meng, Y., and Duffy, T.S. (2014) Phase transitions and equation of state of forsterite to 90 GPa from single-crystal X-ray diffraction and molecular modeling. American Mineralogist, 99, 35–43.

Poe, B.T., Romano, C., Nestola, F., and Smyth, J.R. (2010) Electrical conductivity anisotropy of dry and hydrous olivine at 8 GPa. Physics of the Earth and Planetary Interiors, 181, 103–111.

Zhang, D., Hu, Y., Xu, J., Downs, R.T., Hammer, J.E., and Dera, P.K. (2019) High-pressure behavior of liebenbergite: The most incompressible olivine-structured silicate. American Mineralogist, 104, 580–587.

Zhang, J.S., Hu, Y., Shelton, H., Kung, J., and Dera, P. (2017) Single-crystal X-ray diffraction study of Fe2SiO4 fayalite up to 31 GPa. Physics and Chemistry of Minerals, 44, 171–179.

Zhang, L. (1998) Single crystal hydrostatic compression of (Mg,Mn,Fe,Co) 2 SiO 4 olivines. Physics and Chemistry of Minerals, 25, 308–312.